

MIT Open Access Articles

Edge Temperature Gradient as Intrinsic Rotation Drive in Alcator C-Mod Tokamak Plasmas

The MIT Faculty has made this article openly available. **Please share** how this access benefits you. Your story matters.

Citation: Rice, J. et al. "Edge Temperature Gradient as Intrinsic Rotation Drive in Alcator C-Mod Tokamak Plasmas." *Physical Review Letters* 106.21 (2011) © 2011 American Physical Society

As Published: <http://dx.doi.org/10.1103/PhysRevLett.106.215001>

Publisher: American Physical Society

Persistent URL: <http://hdl.handle.net/1721.1/67326>

Version: Final published version: final published article, as it appeared in a journal, conference proceedings, or other formally published context

Terms of Use: Article is made available in accordance with the publisher's policy and may be subject to US copyright law. Please refer to the publisher's site for terms of use.



Edge Temperature Gradient as Intrinsic Rotation Drive in Alcator C-Mod Tokamak Plasmas

J. E. Rice,¹ J. W. Hughes,¹ P. H. Diamond,^{2,3} Y. Kosuga,³ Y. A. Podpaly,¹ M. L. Reinke,¹ M. J. Greenwald,¹
Ö. D. Gürçan,⁴ T. S. Hahm,⁵ A. E. Hubbard,¹ E. S. Marmor,¹ C. J. McDevitt,³ and D. G. Whyte¹

¹PSFC, MIT, Cambridge, Massachusetts 02139, USA

²NFRI, Daejeon 305-333, Korea

³UCSD, San Diego, California 92093, USA

⁴LPP Ecole Polytechnique, 91128, Palaiseau, CEDEX, France

⁵PPPL, Princeton, New Jersey 08543, USA

(Received 2 November 2010; published 23 May 2011)

Intrinsic rotation has been observed in *I*-mode plasmas from the C-Mod tokamak, and is found to be similar to that in *H* mode, both in its edge origin and in the scaling with global pressure. Since both plasmas have similar edge ∇T , but completely different edge ∇n , it may be concluded that the drive of the intrinsic rotation is the edge ∇T rather than ∇P . Evidence suggests that the connection between gradients and rotation is the residual stress, and a scaling for the rotation from conversion of free energy to macroscopic flow is calculated.

DOI: 10.1103/PhysRevLett.106.215001

PACS numbers: 52.30.-q, 52.25.Fi, 52.55.Fa

Understanding the mechanism whereby turbulence drives a macroscopic sheared flow is a classical problem in the physics of self-organization. Efforts to understand this phenomenon have motivated development of mean field theory Reynolds stress closure models for convective and MHD turbulence [1]. In tokamaks, sheared toroidal rotation appears spontaneously, seemingly as a result of turbulence driven self acceleration.

Rotation and its shear play important roles in the suppression of MHD modes [2] and turbulence [3] in tokamak plasmas. Toroidal rotation is predominantly driven by neutral beams in present day tokamaks, but this method will be much less effective in future devices. An alternative approach is to utilize the self-driven flows (intrinsic rotation) which have been widely observed in plasmas without external momentum input [4]. An understanding of this phenomenon is necessary in order to extrapolate confidently to reactors. Since the transport and relaxation of toroidal momentum is due to turbulence (with $\chi_\phi/\chi_i \sim 1$), intrinsic rotation necessarily implies the existence of an agent or element of the momentum flux which can oppose turbulent viscosity. This off-diagonal flux, the residual stress Π^{res} , is likely responsible for driving intrinsic flow [5]. The connection between observed intrinsic rotation and directly measured Π^{res} has been demonstrated in CSDX plasmas [6]. Residual stress may be understood as a momentum flux driven by macroscopic gradients which produces a directed bulk flow by converting radial inhomogeneity to broken k_\parallel symmetry of the fluctuation spectrum. This process resembles an engine, in that the turbulence converts thermodynamic free energy to macroscopic flow [7].

Several questions arise, the first of which is concerned with the driving gradient. This is a subtle question, since the pressure gradient ∇P can drive instabilities, break k_\parallel

symmetry [8] by its contribution to the zonal flow shear $\langle V_E \rangle$, and also quench turbulence [9] via $\langle V_E \rangle$. Other possibilities include ∇T and ∇n . Here, comparison studies of different confinement regimes (*H*- and *I*-mode plasmas) are used to isolate the driving gradient. The link between this gradient and the macroscopic flow is Π^{res} . A simple theory of the intrinsic rotation engine, based on entropy dynamics, is described, and yields a scaling for the intrinsic rotation velocity.

Intrinsic rotation has been found to be well correlated with the plasma stored energy in *H*-mode plasmas [10] in C-Mod and many other devices [4]. This effect is demonstrated in Fig. 1.

Following the *L*- to *H*-mode transition (~ 0.62 s) there were increases in n_e , $T_e(0)$, W_p and $V_{\text{Tor}}(0)$, the latter determined from the Doppler shifts of x-ray lines. Shown for comparison are the time histories for an *I*-mode plasma. Both discharges had $B_T = 5.4$ T and $I_p = 0.8$ MA, with similar target densities and heating power. The main difference was that the *I*-mode plasma was formed with the unfavorable ion $\mathbf{B} \times \nabla \mathbf{B}$ drift direction. There was very little change in n_e in the *I*-mode case, and a larger increase in T_e . The stored energy in these two discharges was very similar, as was the magnitude of $V_{\text{Tor}}(0)$ and velocity profile shape.

I mode is an operational regime [11] which exhibits *H*-mode energy confinement with *L*-mode particle confinement. Shown in Fig. 2 is a comparison of edge profiles from the plasmas of Fig. 1.

Both plasmas display an edge energy transport barrier, as manifested by the pedestals in T_e at 3 mm inside of the last closed flux surfaces. ∇T at this location is the same for both plasmas, about 60 keV/m. Only the *H*-mode discharge has a pedestal in n_e , however; in *I* mode the edge n_e profile is similar to that in *L* mode. That heat and

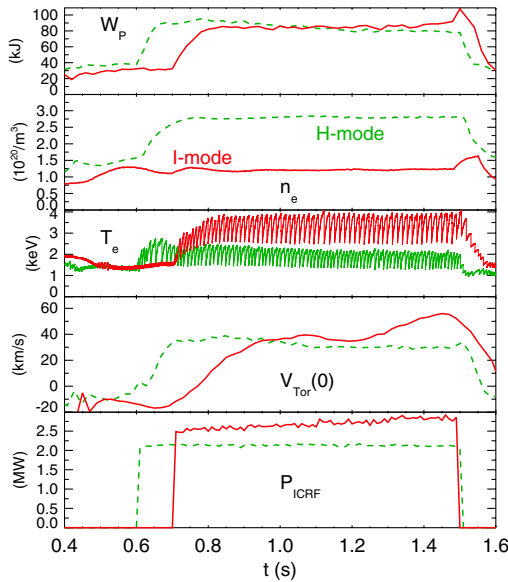


FIG. 1 (color online). Time histories, from top to bottom, of the plasma stored energy, electron density, electron temperature, rotation velocity (positive denotes cocurrent) and ICRF power, for an *H*-mode (green dashed) and an *I*-mode (solid red) plasma.

particle transport is decoupled in *I* mode allows a unique opportunity for energy barriers to be studied separately; in *H* mode both transport channels are usually linked. Since there is no particle barrier in *I* mode, the edge ∇P is considerably lower (~ 0.7 MPa/m, about a factor of 3 in this comparison) compared to *H* mode. The pedestal E_r well depth is also shallower in *I* mode compared to *H* mode [12].

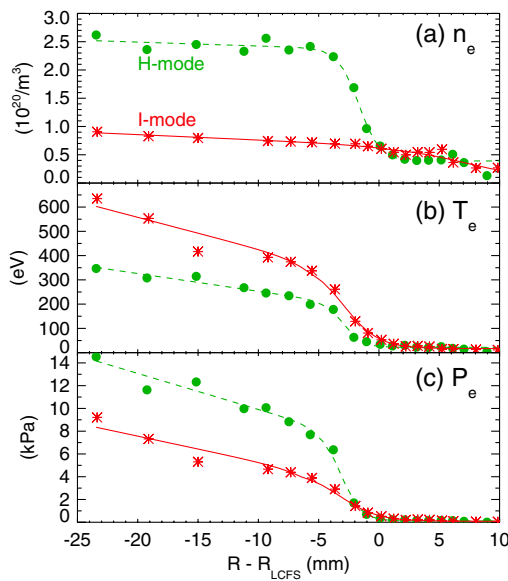


FIG. 2 (color online). Edge profiles of the electron density (a), electron temperature (b) and electron pressure (c) from the *H* mode (green dots) and the *I* mode (red asterisks) discharges of Fig. 1.

For *H*-mode plasmas, it has been established that the intrinsic rotation originates at the plasma edge, and propagates in to the core on a momentum confinement time scale [13]. Similar behavior is seen in *I*-mode plasmas, as shown in Fig. 3.

Following the transition to *I* mode (0.7 s), V_{Tor} first appears at the plasma edge, then propagates in to the plasma center.

It is well documented that the change in V_{Tor} between *L* and *H* mode is proportional to the change in the plasma stored energy (normalized to I_p) [4,10]. Similar behavior is apparent in *I* mode, as can be seen in Fig. 4. The *I*-mode points (red asterisks) overlay the *H*-mode points (green dots) from a large database, suggesting a common phenomenology giving rise to the rotation.

Given the evidence that the origin for the intrinsic rotation is in the pedestal region ([13] and Fig. 3), it would be natural to seek a local edge gradient rather than the global stored energy as relevant to the rotation drive. Intrinsic rotation in JT-60U plasmas has been linked to the ion pressure gradient [14]. Shown in Fig. 5(a) is the change in the rotation velocity as a function of the change in the pedestal ∇P . (In C-Mod plasmas, the edge ion and electron pressure profiles are the same [12].)

For the *H*-mode points, there is a very good correlation between ΔV and edge ∇P . However, the *I*-mode points do not coincide, because the rotation is the same while ∇P is lower than in *H* mode (as seen in Fig. 2). The two sets of points overlay very well for the pedestal ∇T , as demonstrated in Fig. 5(b), suggesting that it is ∇T which is key in driving intrinsic rotation. The association of intrinsic

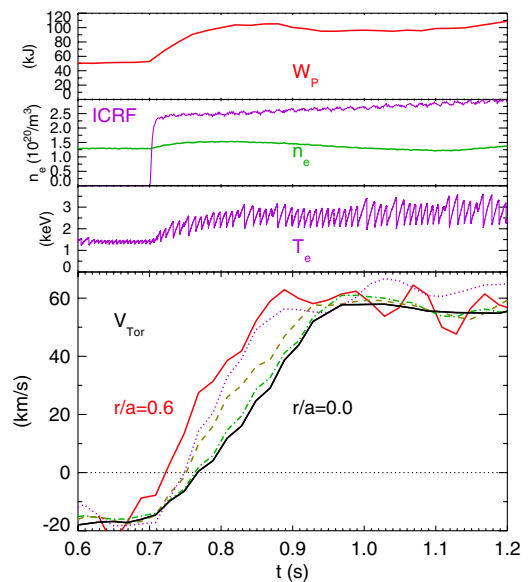


FIG. 3 (color online). Parameter time histories for an *I*-mode discharge. In the bottom frame is the normalized chord-averaged toroidal rotation velocity at several radial locations, evenly spaced from $r/a = 0.6$ to $r/a = 0.0$.

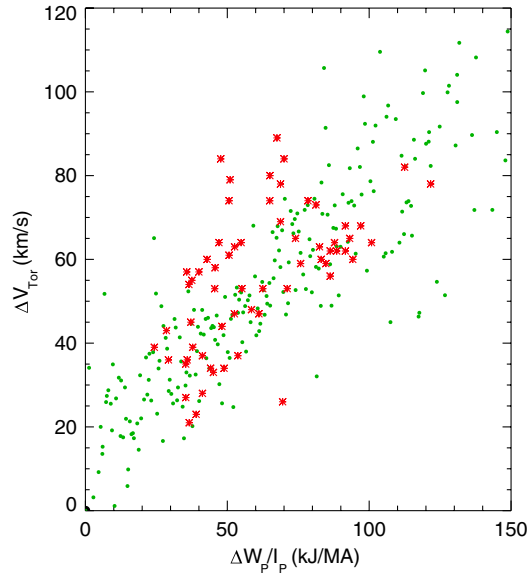


FIG. 4 (color online). The change in the core toroidal rotation from *L* mode to *I* mode (red asterisks) and to *H* mode (green dots) as a function of the change in the stored energy normalized to the plasma current.

rotation with the ion temperature gradient has been demonstrated in LHD ITB plasmas [15].

The approach for addressing the origin of intrinsic flow may be cast in terms of fluctuation entropy and describes intrinsic rotation as a thermodynamic engine. In the framework of residual stress, the flow generation process can be understood as a conversion of thermal energy into the kinetic energy of macroscopic flow by drift wave turbulence excited by ∇T , ∇n , etc. Using the physical picture of flow generation as an energy conversion, an explicit expression for the efficiency of the conversion process may be formulated by comparing rates of entropy production (destruction) due to thermal relaxation (flow) generation [16]. For a model with drift kinetic ions and adiabatic

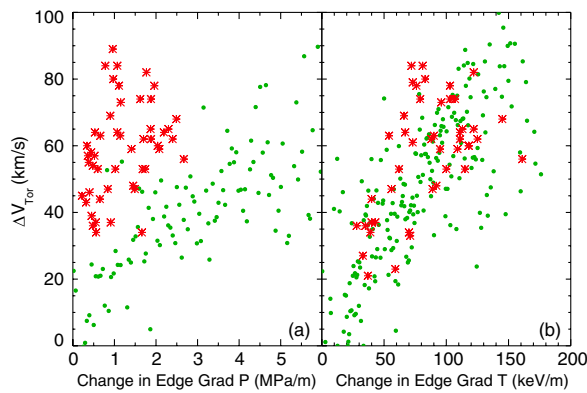


FIG. 5 (color online). The change in the core rotation velocity as a function of the change in the pedestal ∇P (a) and pedestal ∇T (b) for *H*-mode (green dots) and *I*-mode (red asterisks) plasmas.

electrons, the time evolution of entropy or δf^2 is given by, apart from boundary terms,

$$\partial_t \int d^3 v d^3 x \frac{\langle \delta f^2 \rangle}{\langle f \rangle} = P - D_c. \quad (1)$$

Here, $P \equiv \int d^3 x d^3 v \{ -\langle \tilde{V}_r \delta f \rangle \langle f \rangle' / \langle f \rangle - (e/m_i) \langle \tilde{E}_{\parallel} \delta f \rangle / \langle f \rangle (\partial \langle f \rangle / \partial v_{\parallel}) \}$ and $D_c \equiv - \int d^3 x d^3 v \langle \delta f C(\delta f) \rangle / \langle f \rangle$ are the production rate and collisional dissipation of entropy, respectively, following the notation of [16]. Note that the approximation of adiabatic electrons is fairly good, since $\nu_{*e} \sim 1.3 > 1$ and $k_{\parallel}^2 v_{\text{the}}^2 / (\omega \nu_{ei}) \sim 29.6 \gg 1$ for $k_{\perp} \rho_s \sim 0.2$ and for the C-Mod pedestal parameters, $T_i \sim T_e \sim 200$ eV, $q \sim 3$, $\epsilon_A \sim 1/3$, $n \sim 10^{20} \text{ m}^{-3}$. Note also that D_c is small compared to the production rate from ∇T , as $D_c / (n \chi_i / L_T^2) \sim \nu_{\text{eff}} / (c_s / a) \sim 0.08$ where $D_c \sim \int d^3 x n \nu_{\text{eff}} |e \phi / T_e|^2$, $|e \phi / T_e|^2 \sim \rho_s^2$, $\chi_i \sim \chi_{\text{GB}}$ and the same parameters were utilized. Hence D_c is dropped hereafter. By modeling flux-gradient relations, the production rate can be reduced to [16]

$$P \equiv \int d^3 x \left\{ n \chi_i \left(\frac{\nabla T}{T} \right)^2 - n K \left(\frac{\langle V_E \rangle'}{v_{\text{thi}}} \right)^2 + n \chi_{\phi} \left(\frac{\langle V_{\parallel} \rangle'}{v_{\text{thi}}} \right)^2 - n \frac{\Pi_{r\parallel}^{\text{res2}}}{v_{\text{thi}}^2 \chi_{\phi}} \right\} \quad (2)$$

where $K \equiv \sum_k c_s^2 \tau_{\text{ZF}} (\rho_s^2 k_{\theta}^2) / (1 + k_{\perp}^2 \rho_s^2)^2 \{ -k_r \partial \eta_k / \partial k_r \}$, $\eta_k \equiv (1 + k_{\perp}^2 \rho_s^2)^2 |\hat{\phi}_k|^2$. The first term on the right-hand side is the entropy production rate due to thermal relaxation. Note this term is implicitly related to the heat source, as ∇T is tied to heat input via the heat balance equation. The second term is the entropy destruction rate due to zonal flow generation. Note that this term destroys entropy only when zonal flow grows, i.e., $\gamma_{\text{ZF}} \propto K > 0$. The third term is the entropy production rate due to the relaxation of the velocity gradient. The last term is the entropy destruction rate due to the generation of intrinsic toroidal rotation. Entropy production rate by particle transport, namely $-\langle \tilde{V}_r \tilde{n} \rangle \langle n \rangle'$, is small for adiabatic electrons.

The production rate P contains terms with a definite order. The last two terms are smaller than the first two by the order of $O(k_{\parallel} / k_{\perp})$, where k is representative of the mode number of drift waves. Hence a stationary state is achieved by balancing the production and destruction rates order by order. To lowest order, the balance is between the production rate from thermal relaxation and the destruction rate from zonal flow growth. The balance yields $\langle V_E \rangle'^2 = (\chi_i / K) (v_{\text{thi}}^2 / L_T^2)$ which relates zonal flow strength to ∇T directly. To the next order, the third and the fourth terms in Eq. (2) cancel since the total parallel momentum vanishes for a stationary state as $\langle \tilde{V}_r \tilde{V}_{\parallel} \rangle = -\chi_{\phi} \langle V_{\parallel} \rangle' + \Pi_{r\parallel}^{\text{res}} = 0$.

To calculate $\langle V_{\parallel} \rangle'$, a model of the residual stress is required. Here, a case is considered where toroidal rotation is driven by a two step process: first, a stationary state is achieved by balancing the entropy production rate due to

thermal relaxation by the entropy destruction due to zonal flow growth. Secondly, the zonal flow $E \times B$ shear set by the dominant balance gives rise to symmetry breaking and momentum flux via k space scattering. In such a process, the residual stress is calculated as [5,8]

$$\Pi_{r\parallel}^{\text{res}} = -\rho_* \frac{L_s}{2c_s} K \langle V_E \rangle^2 = -\rho_* \frac{L_s}{2c_s} \chi_i \left(\frac{\nabla T}{T} \right)^2 v_{\text{thi}}^2. \quad (3)$$

The condition $\langle \tilde{V}_r, \tilde{V}_{\parallel} \rangle = 0$ implies a strongly nonlinear relation between ∇V_{\parallel} and $\nabla T/T$, i.e.,

$$\langle V_{\parallel} \rangle = \frac{\Pi_{r\parallel}^{\text{res}}}{\chi_{\phi}} = -\frac{1}{2} \rho_* \frac{\chi_i}{\chi_{\phi}} \frac{L_s}{c_s} \left(\frac{\nabla T}{T} \right)^2 v_{\text{thi}}^2. \quad (4)$$

Simple integration then establishes the relation between edge ∇T and the flow velocity,

$$\frac{\langle V_{\parallel} \rangle}{v_{\text{thi}}} \cong \frac{1}{2} \rho_* \frac{\chi_i}{\chi_{\phi}} \frac{L_s}{L_T} \sqrt{\frac{T_i}{T_e}} \propto \frac{\nabla T}{\sqrt{T} I_p}, \quad (5)$$

where $(T'/T)' = -(T'/T)^2 + T''/T \cong -(T'/T)^2$ has been used. The sign conventions here are such that the rotation is predicted to be co-current. For typical H - and I -mode discharges in C -Mod, $\rho_* \sim 0.006$, $T_e \sim T_i$, $\chi_{\phi}/\chi_i \sim 1$, $L_s \sim 0.6$ m and $L_T \sim 0.01$ m, Eq. (5) yields a thermal Mach number of 0.18, which is also typical [4]. Equation (5) captures the ∇T scaling of Fig. 5 from $1/L_T$ and the $1/I_p$ scaling of Fig. 4 from $L_s \propto q/\hat{s} \propto 1/I_p$.

In this Letter, progress toward a physics based phenomenology of intrinsic rotation in H and I mode has been described. The principal results are: there is a close correlation between $\Delta V_T(0)$ and $\nabla T|_{\text{edge}}$, both in H and I mode.

This, in turn, suggests that the macroscopic scaling $\Delta V_T(0) \sim \Delta W_p/I_p$ may be replaced by a relation expressed in terms of *local* parameters, i.e., $\Delta V_T(0) \sim \nabla T/B_{\theta}$. A theory of the entropy balance for a turbulent plasma is presented, which yields a scaling for the residual stress and the toroidal rotation velocity. The theory predicts that V_{\parallel} scales with ∇T and q .

The authors thank the C -Mod operations and ICRF groups for expert running of the tokamak. Work supported by DOE Contract No. DE-FC02-99ER54512 at MIT, DE-AC02-09CH11466 at PPPL and DE-FG02-04ER54738 at UCSD (CMTFO), the W. C. I. program of MEST, Korea and A. N. R. contract ANR-06-PLAN-0084 in France.

-
- [1] U. Frisch *et al.*, *Physica* (Amsterdam) **28D**, 382 (1987).
 - [2] E. J. Strait *et al.*, *Phys. Rev. Lett.* **74**, 2483 (1995).
 - [3] T. S. Hahm, *Phys. Plasmas* **1**, 2940 (1994).
 - [4] J. E. Rice *et al.*, *Nucl. Fusion* **47**, 1618 (2007).
 - [5] P. H. Diamond *et al.*, *Nucl. Fusion* **49**, 045002 (2009).
 - [6] Z. Yan *et al.*, *Phys. Rev. Lett.* **104**, 065002 (2010).
 - [7] Ö. D. Gürçan *et al.*, *Phys. Plasmas* **17**, 032509 (2010).
 - [8] Ö. D. Gürçan *et al.*, *Phys. Plasmas* **14**, 042306 (2007).
 - [9] H. Biglari *et al.*, *Phys. Fluids B* **2**, 1 (1990).
 - [10] J. E. Rice *et al.*, *Nucl. Fusion* **39**, 1175 (1999).
 - [11] D. G. Whyte *et al.*, *Nucl. Fusion* **50**, 105005 (2010).
 - [12] R. M. McDermott *et al.*, *Phys. Plasmas* **16**, 056103 (2009).
 - [13] W. D. Lee *et al.*, *Phys. Rev. Lett.* **91**, 205003 (2003).
 - [14] M. Yoshida *et al.*, *Phys. Rev. Lett.* **100**, 105002 (2008).
 - [15] K. Ida *et al.*, *Nucl. Fusion* **50**, 064007 (2010).
 - [16] Y. Kosuga *et al.*, *Phys. Plasmas* **17**, 102313 (2010).